scientific reports

Check for updates

OPEN

Mechanisms of rifaximin inhibition of hepatic fibrosis in mice with metabolic dysfunction associated steatohepatitis through the TLR4/NFκB pathway

Ting Qiu[1,4,5], Xiaodong Zhu[2,5], Jingju Wu[1], Wenyuan Hong[3], Weitao Hu[1] & Taiyong Fang[1✉]

Metabolic dysfunction-associated steatohepatitis (MASH) has become a serious public health problem, posing an increasingly dangerous threat to human health owing to its increasing prevalence and accompanying intra- and extrahepatic adverse outcomes. Rifaximin is considered to have therapeutic potential for MASH; however, its efficacy remains controversial. Our study aimed to observe the ameliorative effects of rifaximin and explore its possible mechanisms at the cellular level. 1. 42 male C57BL/6J mice were divided into 3 groups, the CON group and MCD group were fed with normal feed and MCD feed for 12 weeks respectively, and the MCD + RFX group was treated with rifaximin by gavage for 4 weeks on the basis of MCD feed. Hematoxylin-eosin staining, Sirius red staining and immunohistochemical staining were used to observe the histopathological changes of liver and intestine. Differences in liver transaminases, inflammatory factors, fibrosis indexes and intestinal tight junction proteins were compared among the 3 groups of mice. 2. A MASH cell model was constructed by inducing HepG2 cells with free fatty acids to observe the effects of rifaximin on MASH in vitro. In addition, the effects of rifaximin on TLR4/NF-κB signaling pathway were explored by applying TLR4 agonist LPS and TLR4 inhibitor TAK-242. Hepatic histopathology was significantly improved in MASH mice after rifaximin treatment, and their serum alanine aminotransferase and aspartate aminotransferase levels were (72.72 ± 5.68) U/L and (222.8 ± 11.22) U/L, respectively, which were significantly lower than those in the MCD group $[(293.3 \pm 10.69)$ U/L and (414.1 ± 36.29) U/L, $P < 0.05]$, and the levels of inflammatory factors and fibrosis indicators were reduced. Rifaximin ameliorated intestinal barrier injury with increased expression of intestinal tight junction protein ZO-1 in the MCD + RFX group of mice, and the concentration of LPS-binding proteins $(4.92 \pm 0.55$ vs. 15.82 ± 1.71, $P < 0.05)$ was lower than that in the MCD group. In the NASH cell model, rifaximin similarly exerted inhibitory effects on its inflammatory factors and TLR4/NF-κB signaling pathway. Application of TLR4 inhibitors weakened the inhibitory effect of rifaximin on MASH. Our study supports rifaximin as a potential treatment for MASH, with potential mechanisms related to improving intestinal barrier integrity and downregulating the TLR4/NF-κB signaling pathway.

Abbreviations

ALT	Alanine aminotransferase
AST	Aspartate aminotransferase
HCC	Hepatocellular carcinoma
IL-1β	Interleukin-1β

[1]Department of Gastroenterology, The Second Affiliated Hospital of Fujian Medical University, Quanzhou, China. [2]Department of Gastroenterology, Quanzhou First Hospital, Quanzhou, China. [3]Anxi Maternal and Child Health Hospital, Quanzhou, China. [4]Present address: Department of General Practice, Longyan First Hospital Affiliated to Fujian Medical University, Longyan, China. [5]Ting Qiu and Xiaodong Zhu contributed equally to this work and shared first authorship. ✉email: fangtaiyong122@126.com

IL-6	Interleukin-6
LPS	Lipopolysaccharide
LBP	Lipopolysaccharide-binding protein
MASLD	Metabolic dysfunction-associated steatotic liver disease
MCD	Methionine-choline deficiency
NAFLD	Non-alcoholic fatty liver disease
MASH	Metabolic dysfunction-associated steatohepatitis
SAF	Steatosis + activity + fibrosis
TNF-α	Tumor necrosis factor-α

Metabolic dysfunction-associated steatotic liver disease (MASLD), once named non-alcoholic fatty liver disease (NAFLD), is a chronic liver disease associated with metabolic dysfunction with abnormal fat deposition in hepatocytes as the main pathological change, with a spectrum of diseases ranging from simple fatty liver to metabolic dysfunction-associated steatohepatitis (MASH) such that a portion of the disease ultimately develops into cirrhosis and even evolution to hepatocellular carcinoma[1]. An estimated 30% of patients with MASLD develop MASH, which is histologically characterized by hepatocellular injury and inflammation with varying degrees of fibrosis[2]. The leading cause of death in patients with MASH is cardiovascular disease, followed by extrahepatic malignancies and liver-related events[3]. The risk of hepatic complications and death increases mainly with increasing liver fibrosis[4,5]; therefore, slowing or reversing fibrosis is important.

The "multiple strikes" theory[6] suggests that MASLD progresses to MASH due to a number of interacting factors, such as endoplasmic reticulum stress, lipotoxicity, insulin resistance, oxidative stress, and even endotoxins from gut microbes, which affect intracellular inflammatory signaling[6–10] and may be potential therapeutic targets. The progression of MASH fibrosis is associated with recurrent inflammatory episodes and anti-inflammatory alternations; thus, suppressing the inflammatory response is critical in protecting against MASLD and MASH[11]. Deficiency in intestinal barrier integrity may predispose patients to hepatic inflammation and promote MASH progression[12]. As the intestinal barrier is compromised, intestinal permeability increases, and a large number of bacteria and related metabolites, such as lipopolysaccharide (LPS), enter the liver via the portal vein[13]. Subsequently, with continued exposure to harmful substances of intestinal origin, the liver sustains damage[14], resulting in the secretion of high levels of cytokines and chemokines by inflammatory and parenchymal cells, such as interleukin-6 (IL-6), tumor necrosis factor-α (TNF-α), and interleukin-1β (IL-1β), which leads to the aggregation of inflammatory cells and the amplification of inflammatory responses[15,16]. The binding of LPS from intestinal translocation to Toll-like receptor 4 (TLR4) induces the release of cytokines from macrophages. It may also activate specific intracellular pathway cascade reactions such as TLR4/NF-κB, resulting in the release of substantial inflammatory mediators. This further aggravates liver injury and plays a significant role in hepatic fibrosis[17–19] (Fig. 1).

Rifaximin, a semi-synthetic derivative of rifamycin SV, has been employed to treat a variety of gastrointestinal disorders with good resistance and a low incidence of adverse effects[20]. However, its efficacy in the treatment of
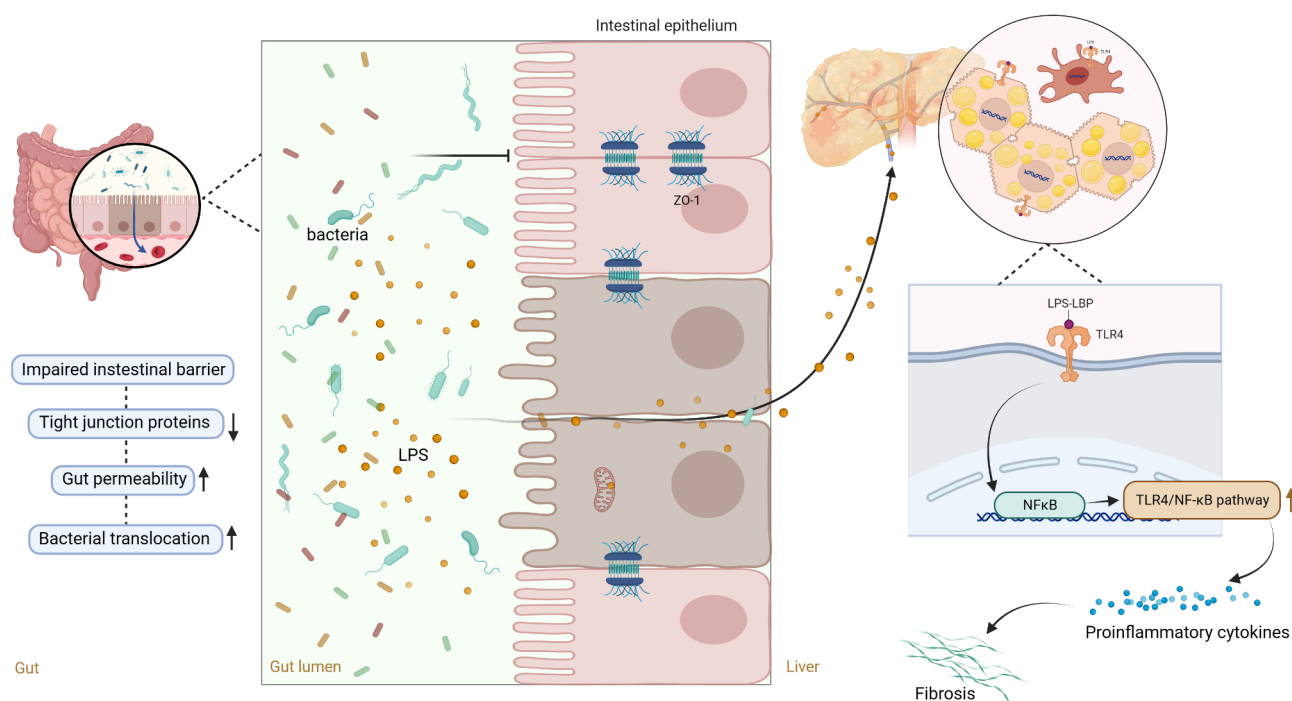

Fig. 1. Illustration of the enterohepatic circulation and the progression of metabolic dysfunction-associated steatohepatitis and liver fibrosis.

MASLD remains controversial. Gangarapu et al.[21] reported that rifaximin inhibits endotoxin pro-inflammatory cytokine production by reducing LPS in patients with MASLD. The anti-fibrotic effects of rifaximin have also been reported[22,23], suggesting that the mechanism may involve a reduction in endogenous LPS overload based on the repair of intestinal barrier integrity[23]. However, Cobbold et al.[24] suggested no therapeutic effect of rifaximin in MASH, as evidenced by an increase in serum ALT levels and insulin resistance in patients with MASH after rifaximin treatment and no significant change in the relative abundance of fecal microbiota. Given the inconclusive role of rifaximin in MASLD, further studies are necessary to confirm its therapeutic efficacy, and its underlying mechanisms require further exploration. We evaluated the effects of rifaximin on hepatic pathological injury, intestinal barrier function, inflammatory response, and fibrosis in MASH and further explored the underlying mechanisms through in vivo and in vitro experiments.

Materials and methods

Animal intervention

C57BL/6J male mice aged 6–8 weeks were purchased from Beijing Huafukang Biotechnology Co., Ltd. Diseased mice were excluded. All animal experiments in this study were conducted in accordance with the ARRIVE guidelines[25] for reporting experiments involving animals. All methods were carried out in accordance with relevant guidelines and regulations. As shown in Fig. 2, mice were randomly divided into two groups according to the random number table method: a control group fed a normal diet (CON group, $n = 15$) and a model group fed a methionine-choline-deficient (MCD) diet (MCD group, $n = 27$). After 8 weeks, each group sacrificed three mice to verify whether MASH was successfully induced. The remaining mice in the CON group ($n = 12$) were fed a normal diet for 4 weeks with saline gavage. The other 24 mice were mechanically classified into two groups: the MCD group ($n = 12$), which continued to be fed MCD food with saline gavage for 4 weeks, and the MCD + RFX group ($n = 12$), which continued to be fed MCD food with rifaximin (50 mg/kg/day) for 4 weeks. Rifaximin (Cat# HY-13234) was purchased from MedChemExpress (www.MedChemExpress.cn). Following the instructions, rifaximin was dissolved by adding 10% DMSO, 40% PEG300, 5% Tween-80 and 45% Saline sequentially. Since the body weight of MCD-fed mice decreases gradually, limited by the maximum gavage volume (40 mL/kg) and rifaximin solubility, and in combination with the rifaximin dosage reported in previous studies, we set the rifaximin dosage administered at 50 mg/kg/day. All mice were housed in the Laboratory Animal Center with free access to food and water, and the circadian rhythm of room temperature was strictly regulated by the animal house staff. After the conclusion of the experiment, mice were euthanized by cervical dislocation following intraperitoneal injection of 1% sodium pentobarbital anesthesia, and blood, liver and intestinal tissues were collected.

Cell culture

HepG2 cells (CL-0103) derived from Wuhan Pricella Biotechnology Co., Ltd, were cultured in Dubecco's modified Eagle's medium (Cat# 25200072, Gibco, Waltham, MA, USA) containing 10% fetal bovine serum (Cat# G11-70500, Gibco) and 1% penicillin/streptomycin (Gibco) at a temperature of 37 °C and a concentration of 5% CO_2.

Determination of serum biochemical parameters

Blood was collected from the heart of mice and layered by high-speed centrifugation (cence, Hunan, China) at 4 °C and 3000 rpm for 15 min to collect the upper serum layer. Serum alanine aminotransferase (ALT) and aspartate aminotransferase (AST) levels were assessed using the ALT (Cat# C009-2-1, Nanjing Institute of Construction Bioengineering, China) and AST assay kits (Cat# C010-2-1, Nanjing Institute of Construction Bioengineering, China). IL-6 and lipopolysaccharide-binding protein (LBP) levels were measured using ELISA kits (Shanghai Jianglai Biotechnology Co. Ltd.).

H&E staining analysis

Following fixation with 4% paraformaldehyde, liver and intestinal tissues were embedded in paraffin. After the tissue sections were prepared, an H&E staining kit (C0105M, Beyotime, Jiangsu, China; G1120, Solarbio, Beijing, China) was used. The pathological findings of the liver were observed under an inverted microscope (IX71, Olympus, Japan). To facilitate quantitative analysis and statistical analysis of liver pathology results, the steatosis + activity + fibrosis (SAF) scoring system proposed by the European Association of Liver Diseases in 2015[26] was used to score the degree of steatosis, inflammatory activity, and fibrosis in each group of mice. When steatosis, ballooning, and lobular inflammation were all scored ≥ 1, the lesion was classified as MASH.

Histology and immunohistochemistry

After removing paraffin, 4 μm thick tissue sections were stained with Sirius red staining solution, followed by a series of ethanol dehydrations starting at 75%, xylene transparency, and finally sealed for microscopic examination. Tissue sections were deparaffinized before antigen repair, titrated with endogenous peroxidase blocker and blocking solution, and immunohistochemically stained with anti-ZO-1 and α-SMA primary antibodies (1:200, Affinity, Cincinnati, OH, USA), followed by incubation with secondary antibodies. After DAB staining, sections were viewed under an inverted microscope. Stained areas were semi-quantified using the ImageJ software (National Institutes of Health, USA).

CCK8 assay

HepG2 cells were cultured in 100 μl culture solution, with five replicate wells in each group. Rifaximin or free fatty acids (FFAs) at different concentrations were added after cell attachment. In the FFAs, the ratio of oleic acid (OA) to palmitic acid (PA) was 2:1. OA (monounsaturated fatty acid, $CH_3(CH_2)_7CH = CH(CH_2)_7COOH$) and
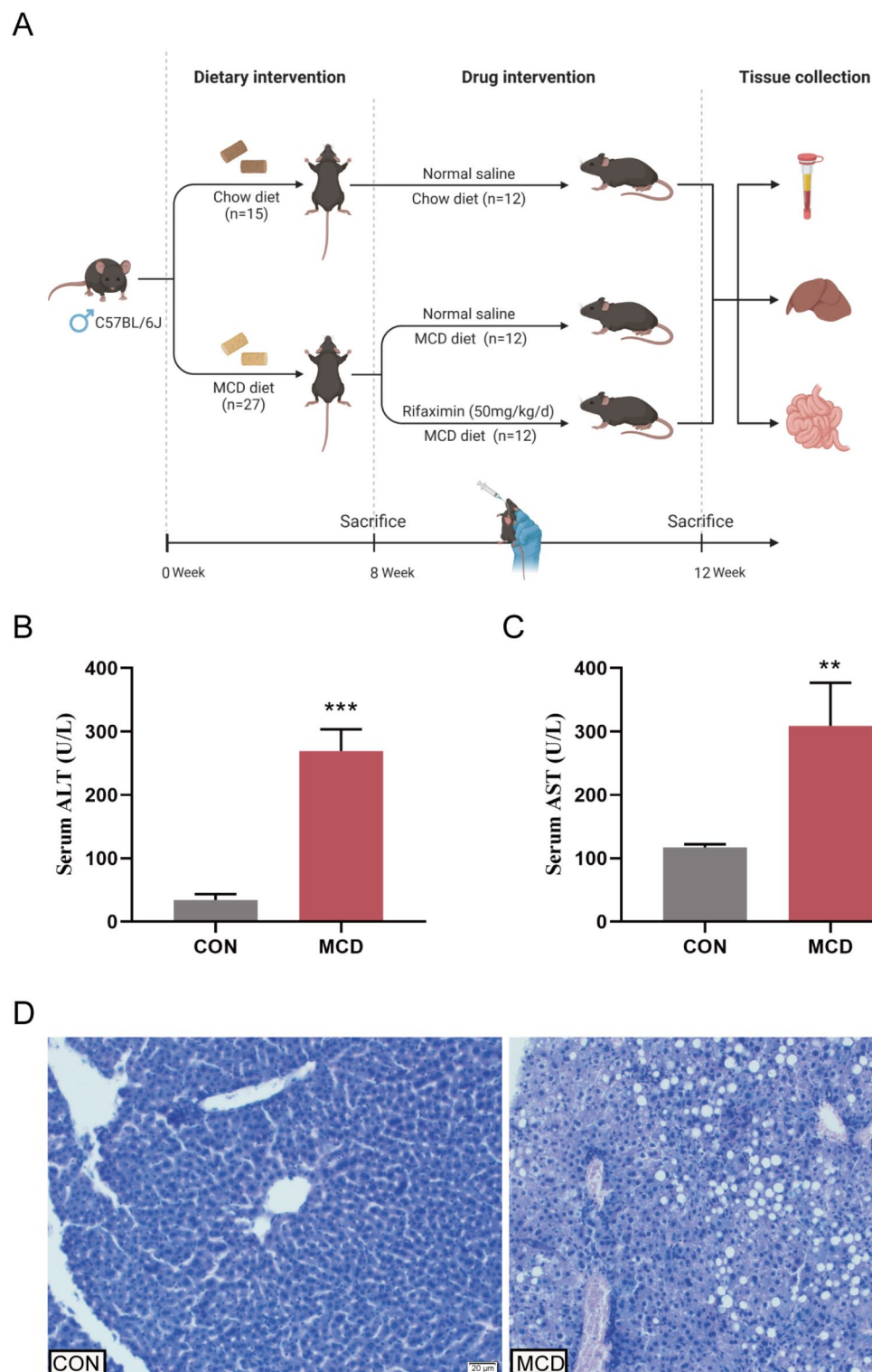
Fig. 2. Panel (**A**), diagram of grouping and interventions of mice. Panel (**B–D**), changes in ALT and AST levels and H&E staining of livers (scale of 20 μm) in mice after 8 weeks of methionine-choline deficiency (MCD) dietary intervention. $^{**}P < 0.01$, $^{***}P < 0.001$ compared with the CON group.

PA (saturated fatty acid, CH3(CH2)14COOH) were purchased from Sigma-Aldrich (Shanghai) Trading Co.Ltd. Following 24 h of incubation in an incubator, 10 μl of CCK-8 solution was added, and incubation was continued for a further period of time before the absorbance at 450 nm was measured using a microplate reader (Scientific Multiskan Sky, Singapore).

Genes	Primer sequences(5'→3')
GAPDH	F: CATGGCCTTCCGTGTTCCTA
	R: GCGGCACGTCAGATCCA
TLR4	F: AGCTTCTCCAATTTTTCAGAACTTC
	R: TGAGAGGTGGTGTAAGCCATGC
NF-κB	F: GCTGCCAAAGAAGGACACGACA
	R: GGCAGGCTATTGCTCATCACAG
ZO-1	F: ACCGGAGAAGTTTCGAGAGC
	R: CTGTACTGTGAGGGCAACGG
LBP	F: AACATCCGGCTGAACACCAAG
	R: CAAGGACAGATTCCCAGGACTGA
IL-6	F: TACCACTTCACAAGTCGGAGGC
	R: CTGCAAGTGCATCATCGTTGTTC
IL-1β	F: TGGACCTTCCAGGATGAGGACA
	R: GTTCATCTCGGAGCCTGTAGTG
α-SMA	F: TGCTGACAGAGGCACCACTGAA
	R: CAGTTGTACGTCCAGAGGCATAG
TGF-β	F: TGATACGCCTGAGTGGCTGTCT
	R: CACAAGAGCAGTGAGCGCTGAA

Table 1. The primer sequences for mice.

Genes	Primer sequences(5' → 3')
TLR4	F: CCCTGAGGCATTTAGGCAGCTA
	R: AGGTAGAGAGGTGGCTTAGGCT
NF-κB	F: GCCTCCACAAGGCAGCAAATA
	R: CACCACTGGTCAGAGACTCGGTAA
IL-6	F: AGACAGCCACTCACCTCTTCAG
	R: TTCTGCCAGTGCCTCTTTGCTG
IL-1β	F: CCACAGACCTTCCAGGAGAATG
	R: GTGCAGTTCAGTGATCGTACAGG
α-SMA	F: CCGGGAGAAAATGACTCAAA
	R: GCAAGGCATAGCCCTCATAG
TGF-β	F: TACCTGAACCCGTGTTGCTCTC
	R: GTTGCTGAGGTATCGCCAGGAA
GAPDH	F: TGCACCACCAACTGCTTAGC
	R: GGCATGGACTGTGGTCATGAG

Table 2. The primer sequences for human HepG2 cells.

Flow cytometry

HepG2 cells were seeded in six-well plates. Following the interventions of FFAs and the TLR4 agonist LPS or the TLR4 inhibitor TAK-242, cell suspensions were supplemented with 5 μl of APC anti-human CD284 (TLR4) or 5 μl of the isotype control antibody APC Mouse IgG2a, κ Isotype Ctrl (FC). Subsequently, cells were incubated 15-minutes in the dark, followed by flow cytometry (NovoCyte, ACEA Biosciences, Hangzhou, China) to determine the TLR4 expression rate on the cell surface.

Real-time quantitative PCR

Total RNA was extracted using the TRIzol reagent (Thermo Fisher Scientific, Waltham, MA, USA), and cDNA was synthesized according to the manufacturer's protocol using a reverse transcription kit (Takara, Kyoto, Japan). The TB Green chimeric fluorescence assay (Takara) was applied for real-time fluorescence quantitative PCR amplification by PCR instrument (Gentier 96E, TIANLONG, Xi'an, China). GAPDH served as the normalization gene. The primer sequences used for the mouse and human HepG2 cells are listed in Tables 1 and 2.

Western blot analysis

Tissues preserved in liquid nitrogen were homogenized in RIPA lysis buffer using an electric homogenizer and an ultrasonic cell crusher, and the supernatant was saved after centrifugation and standardization of the protein concentrations. Proteins in each group were subjected to gel electrophoresis and transferred to polyvinylidene difluoride membranes. Next, the corresponding TLR4, NF-κB, α-SMA, ZO-1, or β-actin primary antibodies

(Affinity) were added and incubated overnight at 4 °C, in addition to incubating with the secondary antibodies (Proteintech, Wuhan, China) for 1 h at room temperature. The assay was performed using an enhanced chemiluminescence detection kit (Yeasen, Shanghai, China).

Statistical analysis
Experimenters conducting outcome assessment and data analysis were blinded. GraphPad Prism 9.5.1 software was used to analyze the data, and measurements were expressed as mean ± standard deviation (SD). A two-sample t-test with a randomized design was applied to compare the experimental and control groups. One-way ANOVA was used for comparisons of more than three samples. $p < 0.05$ was considered a statistically significant difference.

Results
Establishment of the MASH mouse model
To verify the MASH pathological changes in C57BL/6J mice, we sacrificed mice fed for 8 weeks, measured serum ALT and AST levels, and performed H&E staining of liver specimens. Serum ALT (34.1 ± 9.2 vs. 269.0 ± 34.3) and AST (117.3 ± 4.7 vs. 308.7 ± 68.0) were significantly higher in the MCD group ($N = 3$) than in the CON group (Fig. 2B and C). H&E staining (Fig. 2D) showed that hepatocytes in the CON group had normal morphology, the hepatic cords were arranged radially centered on the central vein, and no inflammatory infiltration was observed in the liver, whereas the hepatic cords in the MCD group were significantly disorganized, and moderate steatosis, ballooning, and inflammatory infiltration were identified. These results suggested that the MASH mouse model was successfully constructed.

Effect of rifaximin on liver histopathology in MASH mice
As shown in Fig. 3A and B, the body weights of the mice were significantly reduced from the first week of MCD intervention, and 4 weeks of rifaximin intervention did not result in a noticeable improvement in body size or weight (14.65 ± 0.47 vs. 14.36 ± 0.74). Observation of the livers of mice in each group revealed that the livers of the CON group were reddish brown in color and soft in texture, whereas those of the MCD group were yellowish brown in color, hard in texture, rough on the surface, and accompanied by an oily feeling. The livers of the mice in the MCD + RFX group were light red in color, and their surfaces were smooth (Fig. 3C). Weighing the intact livers (Fig. 3D) revealed no significant alteration in the liver weight (0.55 ± 0.07 vs. 0.62 ± 0.07) and index (liver weight to body weight ratio) (3.86 ± 0.42 vs. 4.21 ± 0.45) in the MCD and MCD + RFX groups of mice. ALT (34.82 ± 7.03 vs. 293.3 ± 10.69) and AST (116.8 ± 7.53 vs. 414.1 ± 36.29) levels were higher in the MCD group ($n = 12$) than in the CON group, whereas they decreased in the MCD + RFX group (ALT 72.72 ± 5.68, AST 222.8 ± 11.22) (Fig. 3E). H&E staining of liver tissue sections revealed that the MCD group had disorganized hepatocytes with unclear lobular boundaries, and the nuclei at the vacuoles shifted to one side. After rifaximin treatment, vacuoles and ballooning were reduced and the morphology of the cell tissues was restored to a certain extent (Fig. 3F). The SAF scoring of H&E-stained sections (Fig. 3G) revealed that mice in the MCD group had considerably higher scores for steatosis, inflammatory responses, balloon-like degeneration, and fibrosis than those in the CON group. These results suggest that rifaximin can alleviate MCD diet-induced pathological changes in the liver of mice.

Effect of rifaximin on inflammatory factors in MASH mice
As shown in Fig. 4A, the IL-6 levels were markedly elevated in the MCD group and decreased after rifaximin treatment. The mRNA levels of IL-6 and IL-1β were distinctly higher in the MCD group, whereas those in the MCD + RFX group were markedly decreased (Fig. 4B and C). Rifaximin has been suggested to reduce inflammation in mice with MASH.

Effect of rifaximin on fibrosis indices in MASH mice
The Sirius red staining results presented in Fig. 4D show that collagen fibers were almost invisible in the CON group, with only a small amount distributed in the vessel wall. The MCD group was characterized by substantial red collagen deposition, with a large amount of expression observed in both the portal vein and the confluent area, and the area of collagen fibers was drastically reduced in the MCD + RFX group. As shown in Fig. 4E and F, expression levels of mRNA for α-SMA and TGF-β showed an increase in the MCD group and a decrease after rifaximin intervention. Similarly, western blotting results showed that α-SMA protein expression was higher in the MCD group and lower in the MCD + RFX group (Fig. 4G and H).

Effect of rifaximin on intestinal barrier integrity in MASH mice
To assess the intestinal barrier integrity in mice, we examined the expression of ZO-1, an intestinal tight junction protein. The expression of LBP, an LPS-binding protein, was examined to assess intestinal permeability. Immunohistochemical results (Fig. 5A and B) showed dramatically reduced ZO-1 expression in the MCD group compared with that in the CON group, whereas ZO-1 expression increased to a certain extent after rifaximin administration. In addition, the ZO-1 mRNA expression and protein content levels were reduced in the MCD group, and rifaximin reversed the decrease in ZO-1 caused by the MCD diet (Fig. 5C–E). Compared with the MCD group, circulating concentrations of LBP (4.92 ± 0.55 vs. 15.82 ± 1.71, $P < 0.05$) and mRNA levels were significantly lower in the MCD + RFX group (Fig. 5F and G). These results indicated that rifaximin improved intestinal barrier integrity and decreased intestinal permeability.
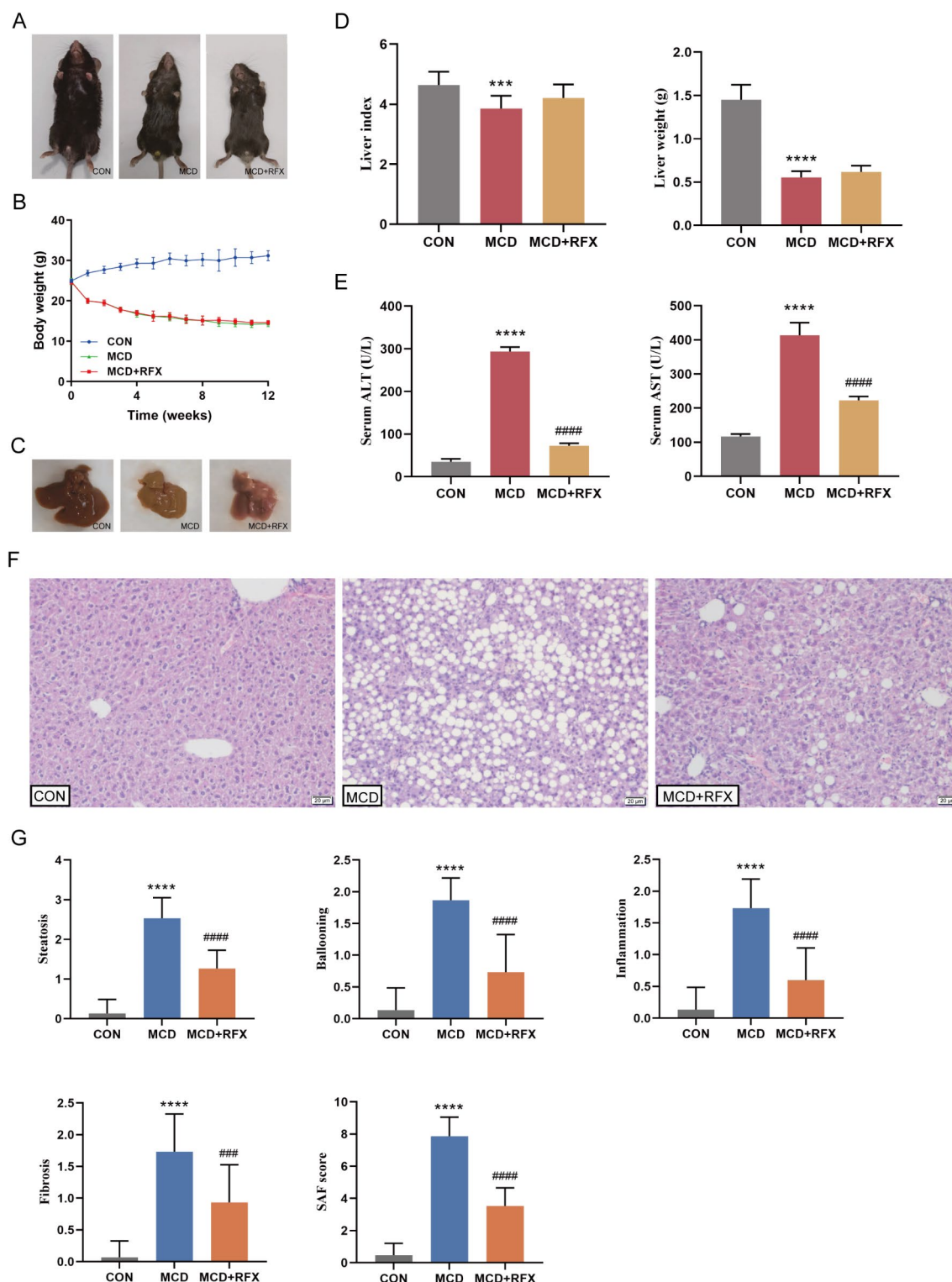
Fig. 3. Effect of rifaximin on liver histopathology. Panel (**A**), appearance of mice. Panel (**B**), growth curves of mice. Panel (**C**), appearance of livers. Panel (**D**), comparison of liver weight and liver index. Panel (**E**), comparison of serum ALT level. Panel (**F**), comparison of H&E staining of livers in each group of mice (scale bar is 20 μm). Panel (**G**), SAF score. ***$P < 0.001$, ****$P < 0.0001$ compared with the CON group. ###$P < 0.001$, ####$P < 0.0001$ compared with the MCD group.
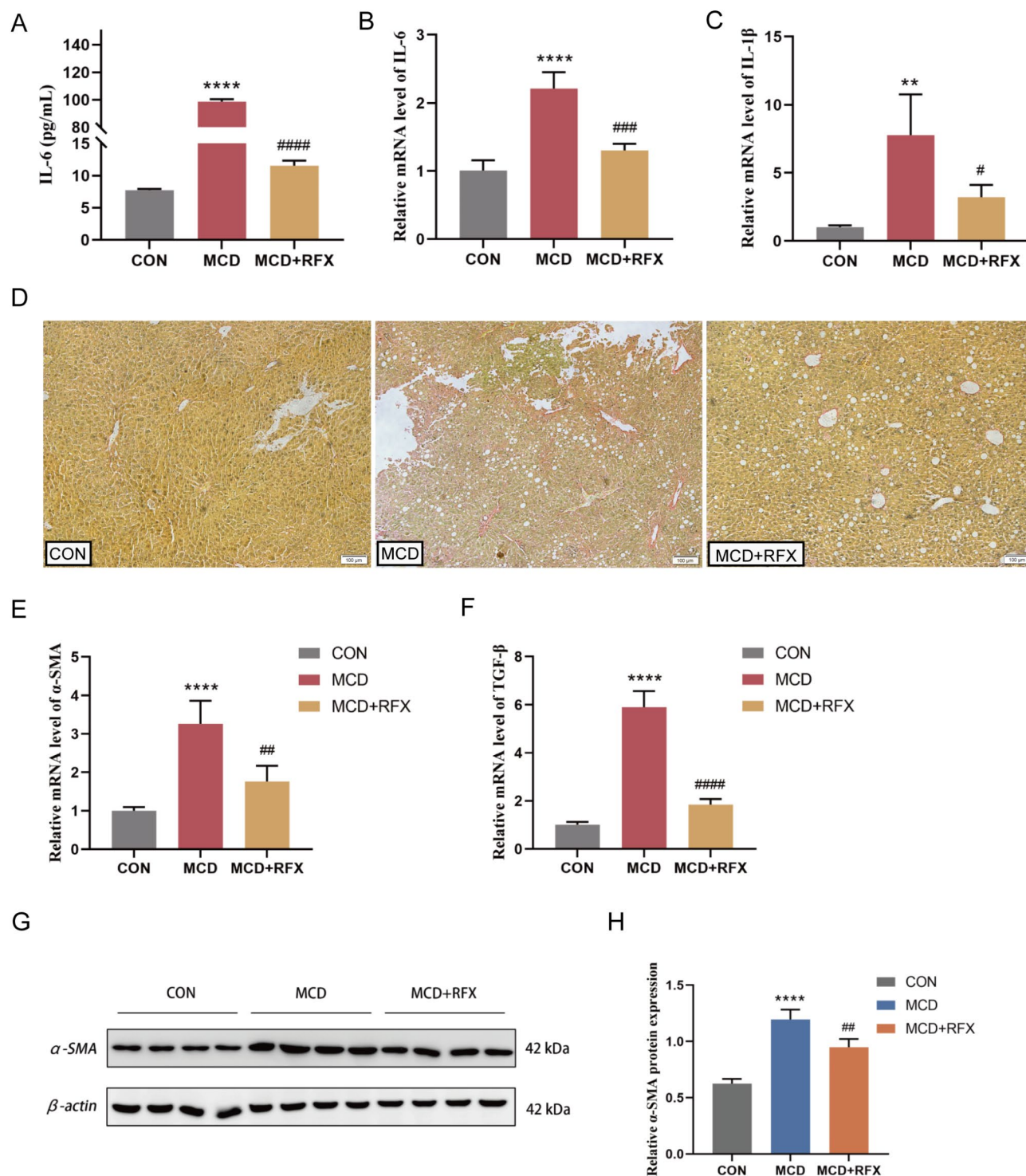
Fig. 4. Effect of rifaximin on inflammatory factors and fibrosis indices. Panel (**A**), serum IL-6 protein level; Panel (**B**), hepatic IL-6 mRNA level; Panel (**C**), hepatic IL-1β mRNA level. Panel (**D**), sirius red staining (scale bar is 100 μm). Panel (**E**), the mRNA levels of α-SMA. Panel (**F**), the mRNA levels of TGF-β. Panel (**G**), the protein expression level of α-SMA. Panel (**H**), semi-quantitative analysis of the α-SMA protein. $^{**}P < 0.01$, $^{****}P < 0.0001$ compared with the CON group. $^{#}P < 0.05$, $^{###}P < 0.001$, $^{####}P<0.0001$ compared with the MCD group.

Effects of rifaximin on the TLR4/NF-κB signaling pathway in MASH mice

The mRNA and protein expression levels of TLR4 and NF-κB were elevated after MCD intervention, which indicated the activation of the TLR4/NF-κB pathway in the liver tissues of the MCD group, whereas rifaximin treatment reduced their expression. (Fig. 6).
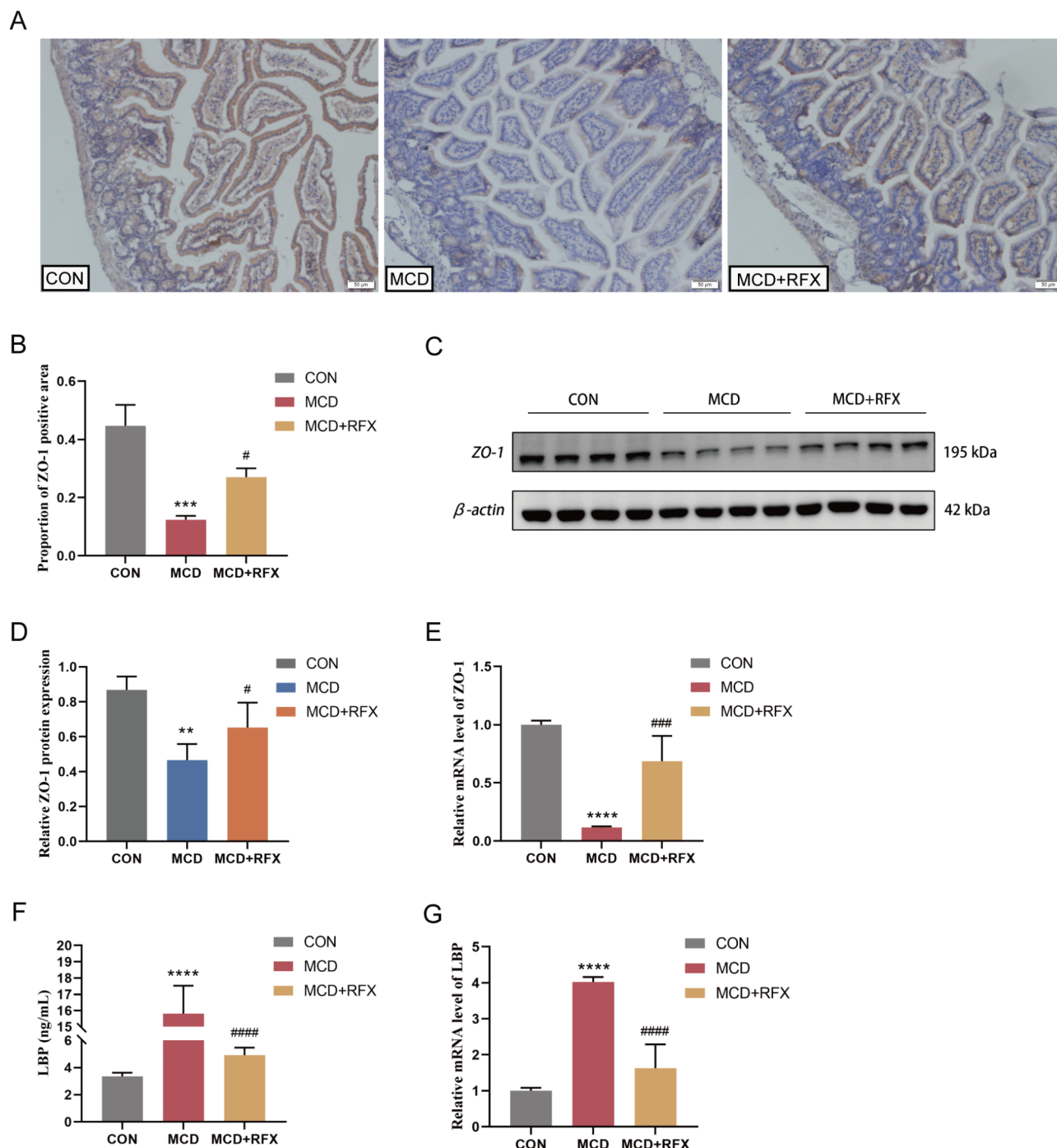
Fig. 5. Effect of rifaximin on intestinal barrier integrity. Panel (**A**), immunohistochemistry of ZO-1 in each group (scale bar is 50 μm). Panel (**B**), semi-quantitative analysis of IHC staining of ZO-1. Panel (**C**), the protein expression level of ZO-1. Panel (**D**), semi-quantitative analysis of ZO-1 protein. Panel (**E**), the mRNA expression level of ZO-1. Panel (**F**), serum LBP concentration. Panel (**G**), the mRNA expression level of LBP. $^{**}P < 0.01$, $^{***}P < 0.001$, $^{****}P < 0.0001$ compared with the CON group. $^{\#}P < 0.05$, $^{\#\#\#}P < 0.001$, $^{\#\#\#\#}P < 0.0001$ compared with the MCD group.

Effects of rifaximin on MASH cell models

In this study, the MASH cell model was induced using FFAs in human liver HepG2 cells. The cytotoxicity of the FFAs was determined. No drug was added to the control group (0 mM), and 0.25, 0.5, 0.75, 1, and 1.25 mM FFAs were administered to each experimental group. As shown in Fig. 7A, the cell survival rate of each dosing group below 1.25 mM was greater than 90%. Therefore, 1 mM FFAs was chosen as the induction concentration for subsequent experiments. Rifaximin cytotoxicity was also determined. The control group (0 μM) cells were not treated with any drug; dimethyl sulfoxide at the same concentration as the experimental group was added
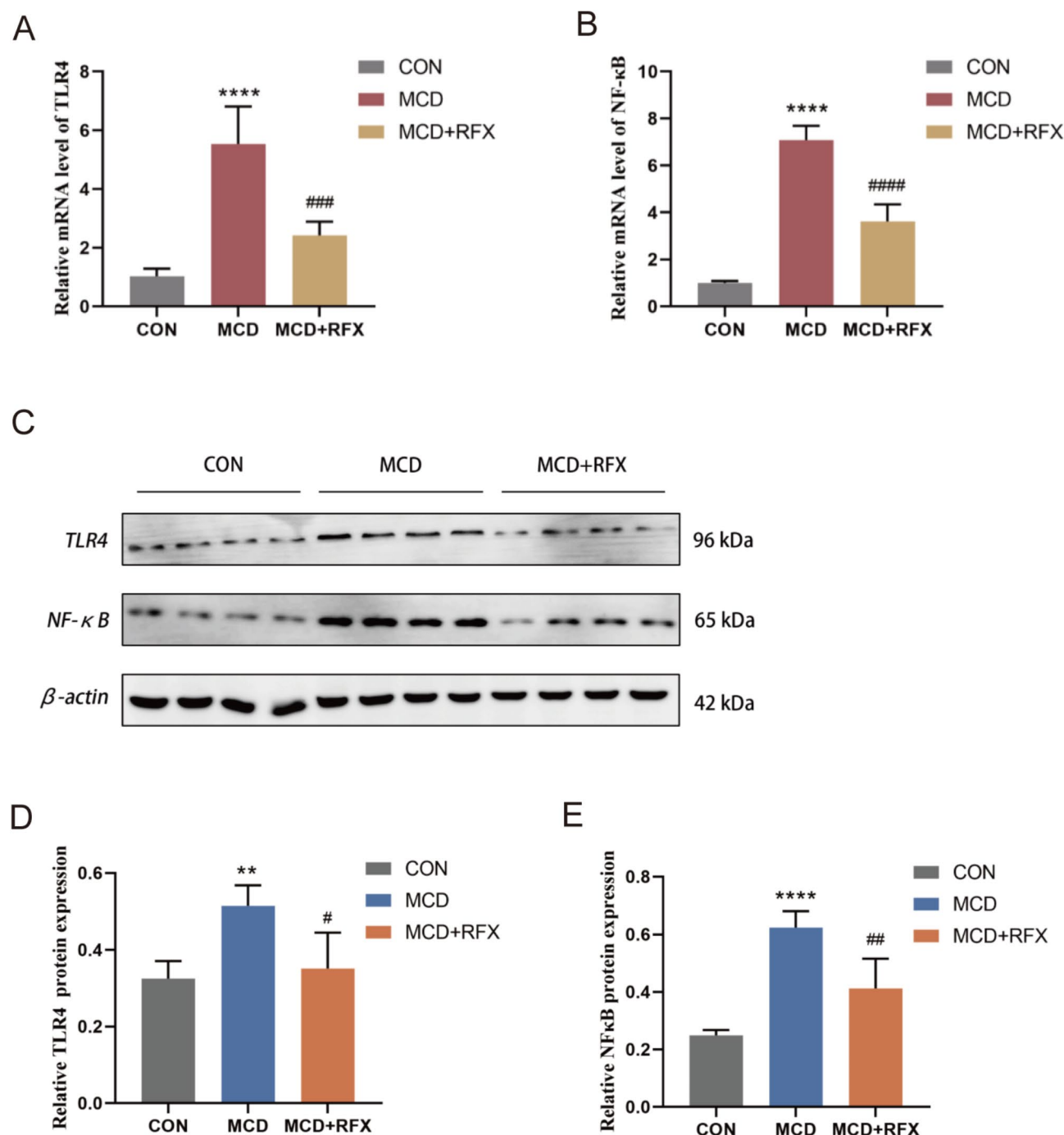
Fig. 6. Effects of rifaximin on the TLR4/NFKB signaling pathway. Panel (**A**), the mRNA expression level of TLR4. Panel (**B**), the mRNA expression level of NFκB. Panel (**C**), the protein expression levels of TLR4 and NF-κB. Panel (**D**), semi-quantitative analysis of TLR4 protein. Panel (**E**), semi-quantitative analysis of NF-κB protein. $^{**}P < 0.01$, $^{****}P < 0.0001$ compared with the CON group. $^{#}P < 0.05$, $^{##}P < 0.01$, $^{###}P < 0.001$, $^{####}P < 0.0001$ compared with the MCD group.

to the medium as a solvent control; and the remaining groups were treated with 25, 50, 75, 100, and 125 μM rifaximin, respectively. The cell viability of the group administered 125 μM concentration was reduced, and the rest of the groups showed no significant difference, indicating good biosafety of rifaximin concentrations < 100 μM (Fig. 7B). We chose 50 μM, 75 μM, and 100 μM as the low, medium, and high dosing concentrations for the next experiments.

The protein and mRNA expression levels of the inflammatory factor IL-6 were elevated in the FFA group as compared with the CON group (Fig. 7C and D), as well as the mRNA level of IL-1β (Fig. 7E). However, rifaximin administration reversed this increasing trend, resulting in a decreasing effect. These results suggest
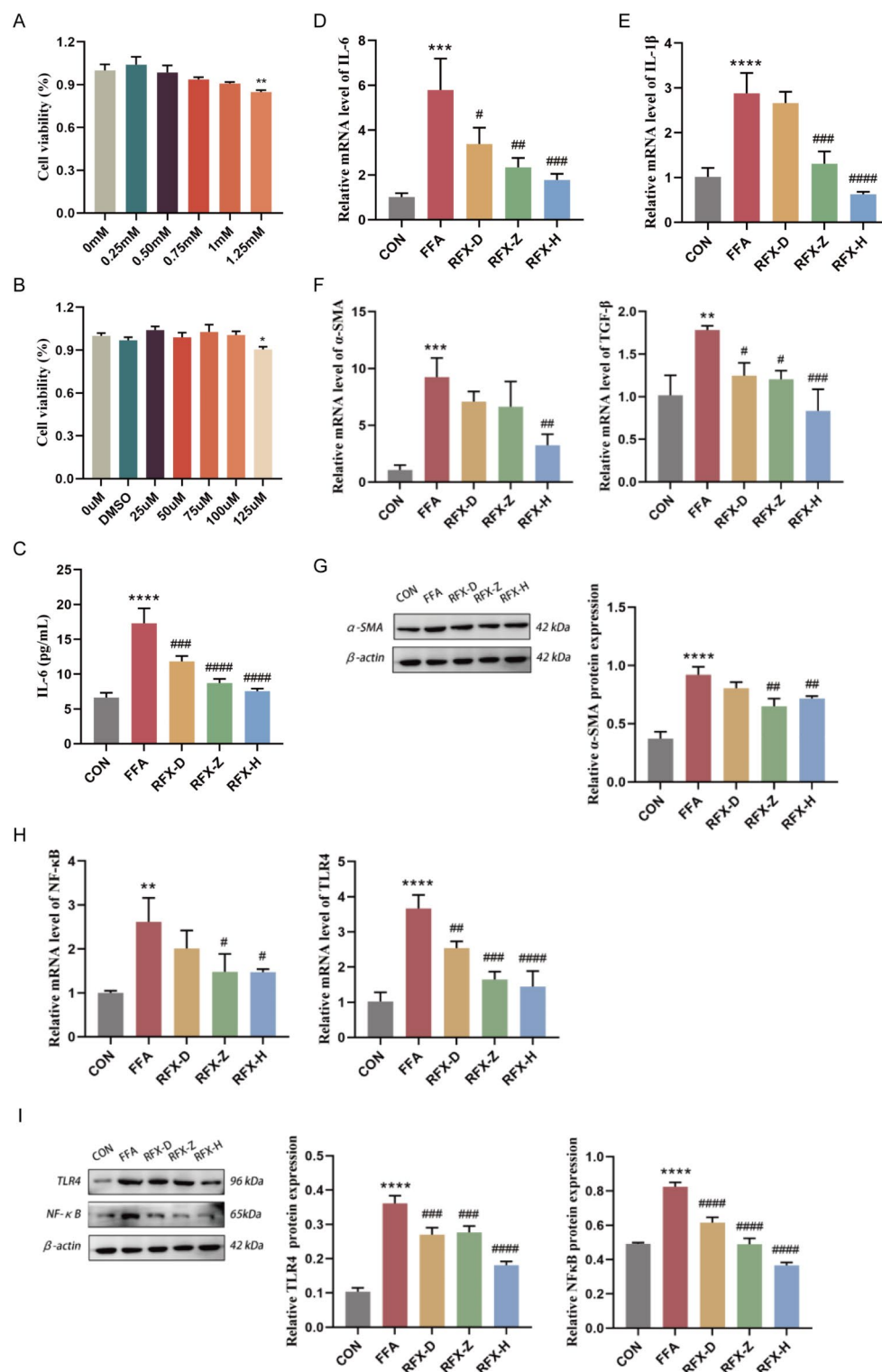
Fig. 7. Effects of rifaximin on MASH cell models. Panel (**A**), effect of free fatty acids on cell viability. Panel (**B**), effect of rifaximin on cell viability. Panel (**C**), serum IL-6. Panel (**D**), the mRNA expression level of IL-6. Panel (**E**), the mRNA expression level of IL-1β. Panel (**F**), the mRNA expression level of α-SMA and TGF-β. Panel (**G**), the protein expression levels of α-SMA. Panel (**H**), the mRNA expression levels of TLR4 and NF-κB. Panel (**I**), the protein expression levels of TLR4 and NF-κB. $^{*}P < 0.05$, $^{**}P < 0.01$, $^{***}P < 0.001$, $^{****}P < 0.0001$ compared with the CON group. $^{\#}P < 0.05$, $^{\#\#}P < 0.01$, $^{\#\#\#}P < 0.001$, $^{\#\#\#\#}P < 0.0001$ compared with the FFA group.
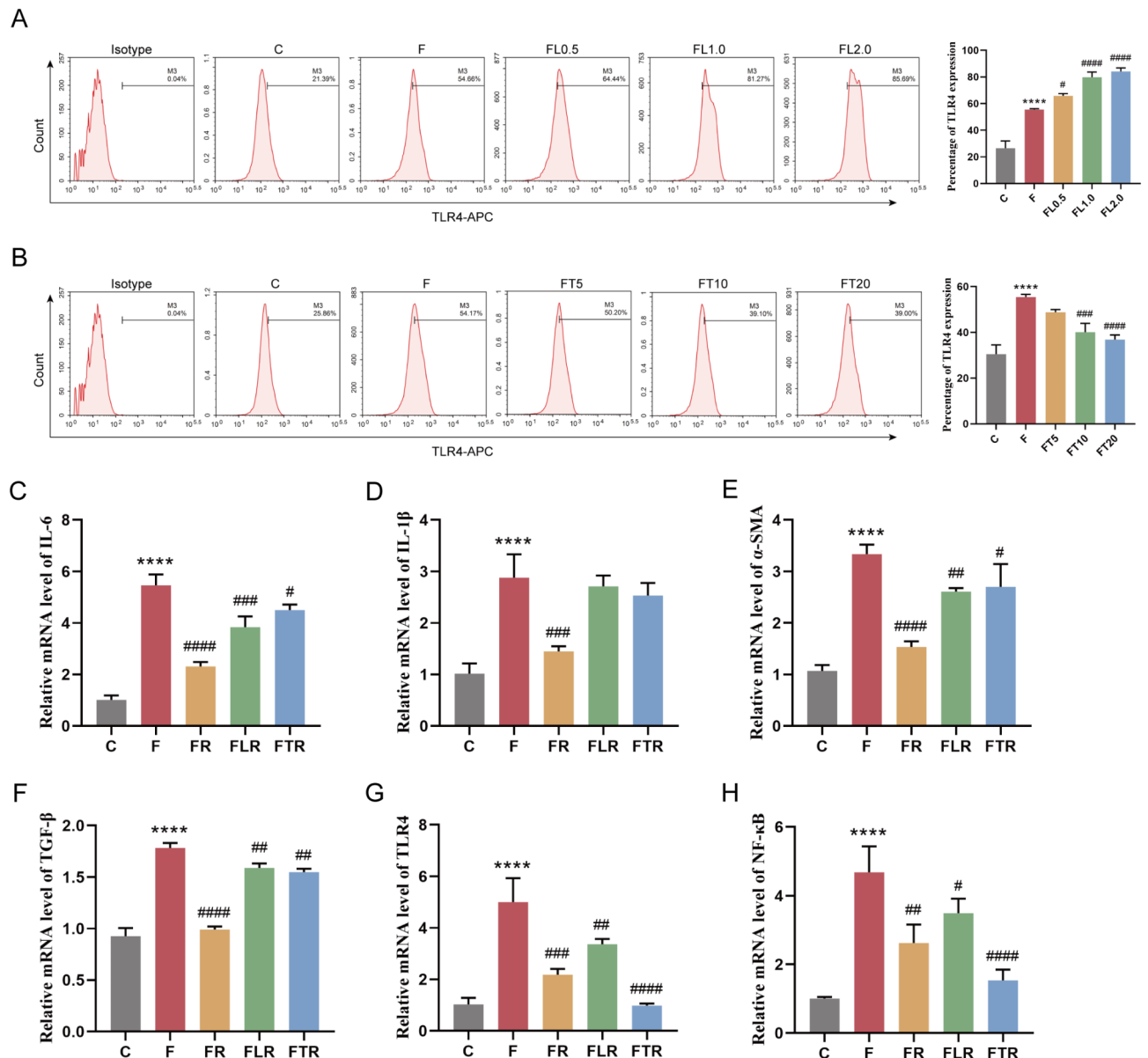
Fig. 8. Rifaximin ameliorates MASH through the TLR4/NF-κB signaling pathway. Panel (**A**), effect of LPS on TLR4 expression rate. Panel (**B**), effect of TAK-242 on TLR4 expression rate detected by flow cytometry. Panel (**C**), the mRNA expression levels of IL-6. Panel (**D**), the mRNA expression levels of IL-1β. Panel (**E**), the mRNA expression levels of α-SMA. Panel (**F**), the mRNA expression levels of TGF-β. Panel (**G**), the mRNA expression levels of TLR4. Panel (H), the mRNA expression levels of NF-κB. $^*P < 0.05$, $^{**}P < 0.01$, $^{***}P < 0.001$, $^{****}P < 0.0001$ compared with the C group. $^{#}P < 0.05$, $^{##}P < 0.01$, $^{###}P < 0.001$, $^{####}P < 0.0001$ compared with the F group.

that rifaximin suppresses inflammation in MASH cell models. The FFAs intervention increased the mRNA levels of α-SMA and TGF-β. Their expression was attenuated by high-dose rifaximin (Fig. 7F). Similarly, western blot showed a significant increase in α-SMA content in the FFA group; the low-dose intervention group (RFX-D) showed a decreasing trend in α-SMA protein expression but no statistical difference; in the medium- and high-dose groups (RFX-Z, RFX-H), the decrease was obvious after rifaximin intervention (Fig. 7G). These results suggested that rifaximin attenuated fibrosis in the MASH cell model. As shown in Fig. 7H and I, the TLR4 and NF-κB mRNA levels as well as protein content were considerably elevated in the FFA group, but were decreased after rifaximin intervention. It has been suggested that rifaximin inhibits the TLR4/NF-κB signaling pathway in a MASH cell model.

Rifaximin ameliorates MASH through the TLR4/NF-κB signaling pathway

The TLR4 expression rate was determined to screen for optimal concentrations of the TLR4 agonist LPS and TLR4 inhibitor TAK-242. As shown in Fig. 8A, the TLR4 expression rate in Isotype group was almost 0; group

C was a normal control group without drug intervention, and the TLR4 expression rate was $26.51 \pm 5.47\%$; group F was a model group administered 1 mM FFAs, and the TLR4 expression rate was $55.46 \pm 0.75\%$, which was a higher TLR4 expression than that of group C; in group FL0.5, LPS 0.5 μg/mL was added based on group F, and the TLR4 expression rate was $65.78 \pm 1.72\%$; in group FL1.0, the concentration of LPS was 1.0 μg/mL, which raised the TLR4 expression rate to $79.77 \pm 3.84\%$; in group FL2.0, the LPS concentration was 2.0 μg/mL, with a TLR4 expression rate of $84.04 \pm 2.72\%$. There was no statistically significant difference in the TLR4 expression rate after LPS treatment at 1.0 and 2.0 μg/mL concentrations. Thus, 1.0 μg/mL LPS was used in the subsequent experiments. In Fig. 8B, the TLR4 expression rate in group C is $30.49 \pm 4.04\%$; in group F, this rate was $55.45 \pm 1.11\%$; in group FT5, TAK-242 5 μmol/mL was added, and the TLR4 expression rate was $48.74 \pm 1.26\%$, which was slightly lower than that of group F; in groups FT10 and FT20, TLR4 expression showed no significant difference. We took 10 μmol/mL as the TAK-242 concentration in the following experiments.

The mRNA levels of IL-6, IL-1β, α-SMA, and TGF-β were increased in the model group (F group) (Fig. 8C–F); these were decreased after rifaximin administration (FR group); the agonist + drug group (FLR group) showed an attenuated effect of rifaximin in downregulating the inflammatory factors and fibrotic indexes; and their mRNA levels were instead greater in the inhibitor + drug group (FTR group) relative to the FR group. This indicated a weakened inhibitory effect of rifaximin on inflammation and fibrosis after TLR4 inhibition. Similarly, the mRNA levels of TLR4 and NF-κB were elevated in group F and declined in group FR; LPS weakened the downregulation of TLR4 and NF-κB by rifaximin in the FLR group; and their mRNA levels were both significantly reduced in group FTR (Fig. 8G and H). The above results suggested that the effect of rifaximin on improving the MASH cell model was related to the regulation of the TLR4/NF-κB signaling pathway.

Discussion

MASH, a progressive form of MASLD, is associated with inflammation and fibrosis, leading to possible progression to cirrhosis, HCC, or even death[15,27,28]. Fibrosis stage is a major prognostic factor for all-cause death[29]. Therefore, treatment of MASH and liver fibrosis is of great importance. Our results showed that rifaximin attenuated liver injury, gut barrier disruption, inflammation, and fibrosis in the MASH model. Based on these results, rifaximin may be used as a treatment for MASH and hepatic fibrosis.

Karmen et al.[30] first reported elevated serum ALT and AST levels in patients with liver injury in 1955. ALT and AST levels have become important biomarkers for assessing liver function[31,32]. ALT and AST are mainly distributed within hepatocytes and are released into the bloodstream when hepatocytes are damaged[32]. We harvested serum from mice at 8 and 12 weeks of intervention to test ALT and AST levels, which was consistent with a study by Abdel-Razik et al.[33]. The findings showed a marked increase in ALT and AST levels in the MCD group compared with those in the CON group. In contrast, a noticeable decrease in ALT and AST levels was observed after 4 weeks of rifaximin gavage, suggesting that rifaximin can ameliorate liver injury in MASH mice.

The intestinal barrier represents the first line of defense of the intestinal lumen against potentially harmful substances, with its structural integrity playing a vital role in the maintenance of regular vital activities of the organism and the homeostasis of the internal environment[34,35]. Tight junction proteins are major determinants of intestinal barrier function[36], maintaining the integrity of the intestinal barrier and inhibit paracellular permeability. ZO-1 was the first tight junction protein identified[37]. We observed that intestinal ZO-1 expression was significantly reduced in the MCD group, suggesting that intestinal barrier integrity was disrupted in MASH mice. Rifaximin is believed to alter intestinal flora and modulate intestinal barrier function[38,39]. Similarly, our results suggest that rifaximin treatment can increase ZO-1 expression and restore intestinal integrity. Deficiency of tight junction proteins can lead to increased intestinal permeability and subsequent translocation of bacterial products such as LPS to the liver, thereby predisposing patients to liver inflammation and MASH progression[40,41]. LBP was used to assess circulating LPS levels because it is more difficult to measure by rapid hepatic clearance, and that LBP correlates positively with LPS concentrations[42]. Rifaximin may act as an anti-fibrotic agent by repairing the intestinal barrier and reducing LPS[23]. We found significantly higher serum levels of LBP in the MCD group, whereas rifaximin intervention resulted in the downregulation of LBP concentrations. It was suggested that the permeability of the intestinal barrier was impaired after the reduction of ZO-1, and LPS through the intestinal barrier into the liver via the portal vein was increased, whereas rifaximin reduced LPS.

Inflammation is an independent predictor of advanced fibrosis in patients with MASH[43]. Once liver inflammation occurs in MASH, it persists through a vicious cycle that occurs both extra- and intrahepatically[44]. Targeting the inflammation-reducing pathway is an effective approach for MASH treatment[45]. Interleukin-6 (IL-6), the most typical cytokine associated with inflammation, is found at higher levels in patients with MASLD than in healthy controls[46,47]. Interleukin 1β (IL-1β) has been shown to increase lipid deposition in hepatocytes, regulate inflammatory response and fibrosis, and be associated with MASH[48–50]. In this study, we detected higher levels of IL6 and IL1β in the MCD group. Their expression decreased in the RFX + MCD group, and the inflammatory foci of the inflammatory infiltrate, as seen by H&E staining, were reduced compared with those in the MCD group, indicating that rifaximin improved inflammation in MASH mice.

Liver fibrosis is the hepatic repair response to chronic injury[51,52]. Patients with MASH exhibit varying degrees of fibrosis. Early hepatic fibrosis is a reversible process in which the attenuation or elimination of factors contributing to fibrosis can lead to the regression of hepatic fibrosis[53]. α-smooth muscle actin (α-SMA) serves as a marker of HSC activation[54,55], and its expression increases with the degree of liver fibrosis[56,57]. Transforming growth factor β (TGF-β) is a potent fibrotic signal for the production and remodeling of the ECM by fibroblasts, connective tissues, and epithelial cells[58]. We found that, compared with the CON group, the red collagen fibers around the confluent area and central vein were significantly increased after MCD intervention, and the protein and mRNA expression levels of α-SMA and TGF-β were also markedly elevated. The reduced collagen deposition and α-SMA staining intensity in liver tissue and downregulation of α-SMA and TGF-β expression after rifaximin

administration suggested that rifaximin has an anti-hepatic fibrotic effect, which agrees with the description of rifaximin's effects by Zhu et al.[59].

TLR4 is widely distributed in immune-related cells, in addition to hepatocytes, hepatocyte macrophages, endothelial cells of hepatic blood sinusoids, pancreatic alveolar cells, and other human tissue cells[60,61]. With multiple signaling pathways mediated by TLR4 being involved in MASLD[62,63], TLR4 exerts an influential effect in promoting the evolution of MASH[64,65]. The TLR4/NF-κB signaling pathway regulates hepatocyte apoptosis, hepatic inflammatory response, and fibrotic processes in MASLD[18,62]. Studies have suggested that TLR4/NF-κB inhibition improves MASLD progression[66,67]. In this study, rifaximin reduced the expression levels of TLR4 and NF-κB in the MASH mouse and cell models. To further clarify whether rifaximin ameliorates MASH by modulating the TLR4/NF-κB pathway, we used the TLR4 agonist LPS and the TLR4 inhibitor TAK-242 in the cellular model. The results showed that rifaximin significantly decreased the expression of IL-6, IL-1β, α-SMA, and TGF-β in the model group, but the decreasing trend was reversed after application of the TLR4 agonist LPS, suggesting that LPS could attenuate the protective effect of rifaximin on MASH. Following TAK-242 intervention, TLR4 and NF-κB expression were reduced in the cells, indicating that the TLR4/NF-κB pathway was blocked, and at this time, the inhibitory effect of rifaximin on the indicators of inflammation and fibrosis appeared to be weakened, suggesting that rifaximin acts through the modulation of the TLR4/NF-κB signaling pathway. Bacterial LPS is the main recognition receptor for TLR4, combining with TLR4 on hepatocytes and Kupffer cells in the sinusoidal gap to form a complex upon increased intestinal permeability, which transmits extracellular signals to the cell through intracellular structural domains, leading to NF-κB activation, upregulating proinflammatory cytokines and chemokines[68], and inducing pathological changes such as liver inflammation and fibrosis[60,69,70].

We verified the ameliorative effects of rifaximin on the intestinal barrier and permeability in MASH mice, as well as the therapeutic effects on inflammation and fibrosis in MASH mice and cellular models, and confirmed that rifaximin could modulate the TLR4/NF-κB signaling pathway to ameliorate liver fibrosis in MASH through agonism and inhibition of TLR4. However, this study has some limitations. As the MCD model could not replicate the metabolic profile of human MASLD, the effect of rifaximin on metabolism was not addressed; therefore, comprehensive investigation of the therapeutic effect of rifaximin is needed in more MASLD models. Owing to financial constraints, this study only investigated the changes in intestinal tight junction proteins and intestinal permeability. In the future, we propose analyzing the changes in intestinal microorganisms using sequencing and other methods to further explore the mechanism by which rifaximin improves MASLD.

Conclusion
Taken together, rifaximin exerted therapeutic effects on MASH liver fibrosis by improving intestinal barrier integrity and inhibiting inflammation through the modulation of the TLR4/NF-κB signaling pathway.

Data availability
All data generated or analysed during this study are included in this published article and its supplementary information files.

References
1. Rinella, M. E. et al. A multisociety Delphi consensus statement on new fatty liver disease nomenclature. *J. Hepatol.* **79**(6), 1542–1556. https://doi.org/10.1016/j.jhep.2023.06.003 (2023).
2. Benedict, M. & Zhang, X. Non-alcoholic fatty liver disease: An expanded review. *World J. Hepatol.* **9**(16), 715–732. https://doi.org/10.4254/wjh.v9.i16.715 (2017).
3. Targher, G., Tilg, H. & Byrne, C. D. Non-alcoholic fatty liver disease: A multisystem disease requiring a multidisciplinary and holistic approach. *Lancet Gastroenterol. Hepatol.* **6**(7), 578–588. https://doi.org/10.1016/s2468-1253(21)00020-0 (2021).
4. Unalp-Arida, A. & Ruhl, C. E. Liver fibrosis scores predict liver disease mortality in the United States population. *Hepatology* **66**(1), 84–95. https://doi.org/10.1002/hep.29113 (2017).
5. Rinella, M. E. et al. AASLD practice guidance on the clinical assessment and management of nonalcoholic fatty liver disease. *Hepatology* **77**(5), 1797–1835. https://doi.org/10.1097/hep.0000000000000323 (2023).
6. Tilg, H. & Moschen, A. R. Evolution of inflammation in nonalcoholic fatty liver disease: The multiple parallel hits hypothesis. *Hepatology* **52**(5), 1836–1846. https://doi.org/10.1002/hep.24001 (2010).
7. Machado, M. V. & Diehl, A. M. Pathogenesis of nonalcoholic steatohepatitis. *Gastroenterology* **150**(8), 1769–1777. https://doi.org/10.1053/j.gastro.2016.02.066 (2016).
8. Bessone, F., Razori, M. V. & Roma, M. G. Molecular pathways of nonalcoholic fatty liver disease development and progression. *Cell. Mol. Life Sci.* **76**(1), 99–128. https://doi.org/10.1007/s00018-018-2947-0 (2019).
9. Mantena, S. K. et al. Mitochondrial dysfunction and oxidative stress in the pathogenesis of alcohol- and obesity-induced fatty liver diseases. *Free Radic Biol. Med.* **44**(7), 1259–1272. https://doi.org/10.1016/j.freeradbiomed.2007.12.029 (2008).
10. Musso, G., Cassader, M. & Gambino, R. Non-alcoholic steatohepatitis: Emerging molecular targets and therapeutic strategies. *Nat. Rev. Drug Discov.* **15**(4), 249–274. https://doi.org/10.1038/nrd.2015.3 (2016).
11. Miura, K. & Ohnishi, H. Role of gut microbiota and Toll-like receptors in nonalcoholic fatty liver disease. *World J. Gastroenterol.* **20**(23), 7381–7391. https://doi.org/10.3748/wjg.v20.i23.7381 (2014).
12. Rahman, K. et al. Loss of junctional adhesion molecule A promotes severe steatohepatitis in mice on a diet high in saturated fat, fructose, and cholesterol. *Gastroenterology* **151**(4), 733–746. https://doi.org/10.1053/j.gastro.2016.06.022 (2016). .e12.
13. Li, Q. et al. Gut microbiota disorders aggravate terbuthylazine-induced mitochondrial quality control disturbance and PANoptosis in chicken hepatocyte through gut-liver axis. *Sci. Total Environ.* **913**, 169642. https://doi.org/10.1016/j.scitotenv.2023.169642 (2023).
14. Gao, B., Jeong, W. I. & Tian, Z. Liver: an organ with predominant innate immunity. *Hepatology* **47**(2), 729–736. https://doi.org/10.1002/hep.22034 (2008).

15. Schuster, S. et al. Triggering and resolution of inflammation in NASH. *Nat. Rev. Gastroenterol. Hepatol.* **15**(6), 349–364. https://doi.org/10.1038/s41575-018-0009-6 (2018).

16. Novo, E. et al. The biphasic nature of hypoxia-induced directional migration of activated human hepatic stellate cells. *J. Pathol.* **226**(4), 588–597. https://doi.org/10.1002/path.3005 (2012).

17. Petrasek, J., Csak, T. & Szabo, G. Toll-like receptors in liver disease. *Adv. Clin. Chem.* **59**, 155–201. https://doi.org/10.1016/b978-0-12-405211-6.00006-1 (2013).

18. Dela Peña, A. et al. NF-kappaB activation, rather than TNF, mediates hepatic inflammation in a murine dietary model of steatohepatitis. *Gastroenterology* **129**(5), 1663–1674. https://doi.org/10.1053/j.gastro.2005.09.004 (2005).

19. Luo, M. C. et al. Runt-related transcription factor 1 (RUNX1) binds to p50 in macrophages and enhances TLR4-triggered inflammation and septic shock. *J. Biol. Chem.* **291**(42), 22011–22020. https://doi.org/10.1074/jbc.M116.715953 (2016).

20. Kaji, K. et al. Rifaximin ameliorates hepatic encephalopathy and endotoxemia without affecting the gut Microbiome diversity. *World J. Gastroenterol.* **23**(47), 8355–8366. https://doi.org/10.3748/wjg.v23.i47.8355 (2017).

21. Gangarapu, V. et al. Efficacy of rifaximin on Circulating endotoxins and cytokines in patients with nonalcoholic fatty liver disease. *Eur. J. Gastroenterol. Hepatol.* **27**(7), 840–845. https://doi.org/10.1097/meg.0000000000000348 (2015).

22. Fujinaga, Y. et al. Effective combination therapy of Angiotensin-II receptor blocker and rifaximin for hepatic fibrosis in rat model of nonalcoholic steatohepatitis. *Int. J. Mol. Sci.* **21**(15). https://doi.org/10.3390/ijms21155589 (2020).

23. Enomoto, M. et al. Rifaximin and Lubiprostone mitigate liver fibrosis development by repairing gut barrier function in diet-induced rat steatohepatitis. *Dig. Liver Dis.* **54**(10), 1392–1402. https://doi.org/10.1016/j.dld.2022.04.012 (2022).

24. Cobbold, J. F. L. et al. Rifaximin in non-alcoholic steatohepatitis: An open-label pilot study. *Hepatol. Res.* **48**(1), 69–77. https://doi.org/10.1111/hepr.12904 (2018).

25. McGrath, J. C. & Lilley, E. Implementing guidelines on reporting research using animals (ARRIVE etc.): New requirements for publication in BJP. *Br. J. Pharmacol.* **172**(13), 3189–3193. https://doi.org/10.1111/bph.12955 (2015).

26. EASL-EASD-EASO Clinical practice guidelines for the management of non-alcoholic fatty liver disease. *Diabetologia* **59**(6), 1121–1140. https://doi.org/10.1007/s00125-016-3902-y (2016).

27. Brunt, E. M. et al. Nonalcoholic fatty liver disease. *Nat. Rev. Dis. Primers.* **1**, 15080. https://doi.org/10.1038/nrdp.2015.80 (2015).

28. Bedossa, P. Pathology of non-alcoholic fatty liver disease. *Liver Int.* **37 Suppl 1**, 85–89. https://doi.org/10.1111/liv.13301 (2017).

29. Ekstedt, M. et al. Fibrosis stage is the strongest predictor for disease-specific mortality in NAFLD after up to 33 years of follow-up. *Hepatology* **61**(5), 1547–1554. https://doi.org/10.1002/hep.27368 (2015).

30. Karmen, A., Wroblewski, F. & Ladue, J. S. Transaminase activity in human blood. *J. Clin. Invest.* **34**(1), 126–131. https://doi.org/10.1172/jci103055 (1955).

31. Kim, W. R. et al. Serum activity of alanine aminotransferase (ALT) as an indicator of health and disease. *Hepatology* **47**(4), 1363–1370. https://doi.org/10.1002/hep.22109 (2008).

32. McGill, M. R. The past and present of serum aminotransferases and the future of liver injury biomarkers. *Excli J.* **15**, 817–828. https://doi.org/10.17179/excli2016-800 (2016).

33. Abdel-Razik, A. et al. Rifaximin in nonalcoholic fatty liver disease: Hit multiple targets with a single shot. *Eur. J. Gastroenterol. Hepatol.* **30**(10), 1237–1246. https://doi.org/10.1097/meg.0000000000001232 (2018).

34. Koh, Y. Y. et al. The effect of intestinal permeability and endotoxemia on the prognosis of acute pancreatitis. *Gut Liver.* **6**(4), 505–511. https://doi.org/10.5009/gnl.2012.6.4.505 (2012).

35. Kelly, J. R. et al. Breaking down the barriers: The gut microbiome, intestinal permeability and stress-related psychiatric disorders. *Front. Cell. Neurosci.* **9**, 392. https://doi.org/10.3389/fncel.2015.00392 (2015).

36. Yang, L. et al. Rifaximin alters intestinal microbiota and prevents progression of ankylosing spondylitis in mice. *Front. Cell. Infect. Microbiol.* **9**, 44. https://doi.org/10.3389/fcimb.2019.00044 (2019).

37. Stevenson, B. R. et al. Identification of ZO-1: A high molecular weight polypeptide associated with the tight junction (zonula occludens) in a variety of epithelia. *J. Cell. Biol.* **103**(3), 755–766. https://doi.org/10.1083/jcb.103.3.755 (1986).

38. Lopetuso, L. R. et al. The intriguing role of rifaximin in gut barrier chronic inflammation and in the treatment of Crohn's disease. *Expert Opin. Investig. Drugs.* **27**(6), 543–551. https://doi.org/10.1080/13543784.2018.1483333 (2018).

39. Xu, D. et al. Rifaximin alters intestinal bacteria and prevents stress-induced gut inflammation and visceral hyperalgesia in rats. *Gastroenterology* **146**(2), 484–496. https://doi.org/10.1053/j.gastro.2013.10.026 (2014).

40. Alisi, A. et al. Endotoxin and plasminogen activator inhibitor-1 serum levels associated with nonalcoholic steatohepatitis in children. *J. Pediatr. Gastroenterol. Nutr.* **50**(6), 645–649. https://doi.org/10.1097/MPG.0b013e3181c7bdf1 (2010).

41. Farhadi, A. et al. Susceptibility to gut leakiness: A possible mechanism for endotoxaemia in non-alcoholic steatohepatitis. *Liver Int.* **28**(7), 1026–1033. https://doi.org/10.1111/j.1478-3231.2008.01723.x (2008).

42. Du Plessis, J. et al. Activated intestinal macrophages in patients with cirrhosis release NO and IL-6 that May disrupt intestinal barrier function. *J. Hepatol.* **58**(6), 1125–1132. https://doi.org/10.1016/j.jhep.2013.01.038 (2013).

43. Argo, C. K. et al. Systematic review of risk factors for fibrosis progression in non-alcoholic steatohepatitis. *J. Hepatol.* **51**(2), 371–379. https://doi.org/10.1016/j.jhep.2009.03.019 (2009).

44. Hardy, T. et al. Nonalcoholic fatty liver disease: pathogenesis and disease spectrum. *Annu. Rev. Pathol.* **11**, 451–496. https://doi.org/10.1146/annurev-pathol-012615-044224 (2016).

45. Rius, B. et al. The specialized proresolving lipid mediator Maresin 1 protects hepatocytes from lipotoxic and hypoxia-induced Endoplasmic reticulum stress. *Faseb J.* **31**(12), 5384–5398. https://doi.org/10.1096/fj.201700394R (2017).

46. Duan, Y. et al. Association of inflammatory cytokines with non-alcoholic fatty liver disease. *Front. Immunol.* **13**, 880298. https://doi.org/10.3389/fimmu.2022.880298 (2022).

47. Deng, Y. F. et al. Kinsenoside alleviates inflammation and fibrosis in experimental NASH mice by suppressing the NF-κB/NLRP3 signaling pathway. *Phytomedicine* **104**, 154241. https://doi.org/10.1016/j.phymed.2022.154241 (2022).

48. Miura, K. et al. Toll-like receptor 9 promotes steatohepatitis by induction of interleukin-1beta in mice. *Gastroenterology* **139**(1), 323–347. https://doi.org/10.1053/j.gastro.2010.03.052 (2010).

49. Kamari, Y. et al. Lack of interleukin-1α or interleukin-1β inhibits transformation of steatosis to steatohepatitis and liver fibrosis in hypercholesterolemic mice. *J. Hepatol.* **55**(5), 1086–1094. https://doi.org/10.1016/j.jhep.2011.01.048 (2011).

50. Stienstra, R. et al. Kupffer cells promote hepatic steatosis via interleukin-1beta-dependent suppression of peroxisome proliferator-activated receptor alpha activity. *Hepatology* **51**(2), 511–522. https://doi.org/10.1002/hep.23337 (2010).

51. Aoyama, T., Paik, Y. H. & Seki, E. Toll-like receptor signaling and liver fibrosis. *Gastroenterol. Res. Pract.*. https://doi.org/10.1155/2010/192543 (2010).

52. Hernandez-Gea, V. & Friedman, S. L. Pathogenesis of liver fibrosis. *Annu. Rev. Pathol.* **6**, 425–456. https://doi.org/10.1146/annurev-pathol-011110-130246 (2011).

53. Smith, A., Baumgartner, K. & Bositis, C. Cirrhosis: Diagnosis and management. *Am. Fam Physician.* **100**(12), 759–770 (2019).

54. Trivedi, P., Wang, S. & Friedman, S. L. The power of plasticity-metabolic regulation of hepatic stellate cells. *Cell. Metab.* **33**(2), 242–257. https://doi.org/10.1016/j.cmet.2020.10.026 (2021).

55. Tsuchida, T. & Friedman, S. L. Mechanisms of hepatic stellate cell activation. *Nat. Rev. Gastroenterol. Hepatol.* **14**(7), 397–411. https://doi.org/10.1038/nrgastro.2017.38 (2017).

56. Sanyal, A. J. et al. Cirrhosis regression is associated with improved clinical outcomes in patients with nonalcoholic steatohepatitis. *Hepatology* **75**(5), 1235–1246. https://doi.org/10.1002/hep.32204 (2022).

57. Kim, K. E. et al. Lipocalin-2 activates hepatic stellate cells and promotes nonalcoholic steatohepatitis in high-fat diet-fed Ob/Ob mice. *Hepatology* **77**(3), 888–901. https://doi.org/10.1002/hep.32569 (2023).
58. Massagué, J. & Sheppard, D. TGF-β signaling in health and disease. *Cell* **186**(19), 4007–4037. https://doi.org/10.1016/j.cell.2023.07.036 (2023).
59. Zhu, Q. et al. Intestinal decontamination inhibits TLR4 dependent fibronectin-mediated cross-talk between stellate cells and endothelial cells in liver fibrosis in mice. *J. Hepatol.* **56**(4), 893–899. https://doi.org/10.1016/j.jhep.2011.11.013 (2012).
60. Aderem, A. & Ulevitch, R. J. Toll-like receptors in the induction of the innate immune response. *Nature* **406**(6797), 782–787. https://doi.org/10.1038/35021228 (2000).
61. Roh, Y. S. & Seki, E. Toll-like receptors in alcoholic liver disease, non-alcoholic steatohepatitis and carcinogenesis. *J. Gastroenterol. Hepatol.* **28**(01), 38–42. https://doi.org/10.1111/jgh.12019 (2013).
62. Lu, Y. C., Yeh, W. C. & Ohashi, P. S. LPS/TLR4 signal transduction pathway. *Cytokine* **42**(2), 145–151. https://doi.org/10.1016/j.cyto.2008.01.006 (2008).
63. Das, S. et al. Oxidase-Derived peroxynitrite drives inflammation in mice and human nonalcoholic steatohepatitis via TLR4-Lipid raft recruitment. *Am. J. Pathol.* **185**(7), 1944–1957. https://doi.org/10.1016/j.ajpath.2015.03.024 (2015).
64. Shi, H. et al. Chlorogenic acid reduces liver inflammation and fibrosis through Inhibition of toll-like receptor 4 signaling pathway. *Toxicology* **303**, 107–114. https://doi.org/10.1016/j.tox.2012.10.025 (2013).
65. Wenzel, P. et al. Redox regulation of cardiovascular inflammation - Immunomodulatory function of mitochondrial and Nox-derived reactive oxygen and nitrogen species. *Free Radic Biol. Med.* **109**, 48–60. https://doi.org/10.1016/j.freeradbiomed.2017.01.027 (2017).
66. Csak, T. et al. Deficiency in myeloid differentiation factor-2 and toll-like receptor 4 expression attenuates nonalcoholic steatohepatitis and fibrosis in mice. *Am. J. Physiol. Gastrointest. Liver Physiol.* **300**(3), G433–G441. https://doi.org/10.1152/ajpgi.00163.2009 (2011).
67. Yang, L. et al. Differentially regulates hepatic steatosis and inflammation/fibrosis in mice. *Cell. Mol. Gastroenterol. Hepatol.* **3**(3), 469–483. https://doi.org/10.1016/j.jcmgh.2016.12.004 (2017).
68. Spruss, A. et al. Toll-like receptor 4 is involved in the development of fructose-induced hepatic steatosis in mice. *Hepatology* **50**(4), 1094–1104. https://doi.org/10.1002/hep.23122 (2009).
69. Kiziltas, S. Toll-like receptors in pathophysiology of liver diseases. *World J. Hepatol.* **8**(32), 1354–1369. https://doi.org/10.4254/wjh.v8.i32.1354 (2016).
70. Baumann, A. et al. Toll-like receptor 1 as a possible target in non-alcoholic fatty liver disease. *Sci. Rep.* **11**(1), 17815. https://doi.org/10.1038/s41598-021-97346-9 (2021).

Acknowledgements

Author contributions

T.Q. and X.Z. conceived and designed the study, performed the statistical analysis, and drafted the manuscript. J.W., W.H. (Wenyuan Hong), and W.H. (Weitao Hu) revised the manuscript and provided suggestions. T.F. reviewed and edited the manuscript. All authors contributed to the article and approved the submitted version.

Funding

Declarations

Competing interests

The authors declare no competing interests.

Ethics declaration

This study was reviewed and approved by [the Medical Ethics Committee of the Second Affiliated Hospital of Fujian Medical University] with the approval number: [251], dated [May 27, 2022].

Additional information

Supplementary Information The online version contains supplementary material available at https://doi.org/10.1038/s41598-025-92282-4.

Correspondence and requests for materials should be addressed to T.F.

Reprints and permissions information is available at www.nature.com/reprints.

Publisher's note Springer Nature remains neutral with regard to jurisdictional claims in published maps and institutional affiliations.